J. Fluid Mech. (1983), *vol.* 133, *pp.* 47–63
Printed in Great Britain

Propagation of obliquely incident water waves over a trench

By JAMES T. KIRBY AND ROBERT A. DALRYMPLE
Department of Civil Engineering, University of Delaware, Newark, DE 19711

(Received 30 August 1982 and in revised form 18 March 1983)

The diffraction of obliquely incident surface waves by an asymmetric trench is investigated using linearized potential theory. A numerical solution is constructed by matching particular solutions for each subregion of constant depth along vertical boundaries; the resulting matrix equation is solved numerically. Several cases where the trench-parallel wavenumber component in the incident-wave region exceeds the wavenumber for freely propagating waves in the trench are investigated and are found to result in large reductions in wave transmission; however, reflection is not total owing to the finiteness of the obstacle.

Results for one case are compared with data obtained from a small-scale wave-tank experiment. An approximate solution based on plane-wave modes is derived and compared with the numerical solution and, in the long-wave limit, with a previous analytic solution.

1. Introduction

The problem of the diffraction of incident waves by a finite obstacle in an otherwise infinite and uniform domain remains of general interest in linear wave theory. Several geometries of interest can be schematized by domains divided into separate regions by vertical geometrical boundaries, with the fluid depth being constant in each subdomain. Representative two-dimensional problems, with the boundary geometry uniform in the direction normal to the plane of interest, include those of elevated rectangular sills, fixed or floating rectangular obstacles at the water surface, and submerged trenches. The approach to the solution of problems of this type has typically been to construct solutions for each constant-depth subdomain in terms of eigenfunction expansions of the velocity potential; the solutions are then matched at the vertical boundaries, resulting in sets of linear integral equations which must be truncated to a finite number of terms and solved numerically. One of the earliest solutions of this type was given by Takano (1960), who studied the cases of normal wave incidence on an elevated sill and fixed obstacle at the surface. In this study, we employ a modification of Takano's method, discussed in §3. Newman (1965*b*) also employed an integral-equation approach to study reflection and transmission of waves normally incident on a single step between finite- and infinite-depth regions. A variational approach, developed by Schwinger to study discontinuities in waveguides (see Schwinger & Saxon 1968) has been used by Miles (1967), to study Newman's single-step problem, and by Mei & Black (1969), who studied the symmetric elevated sill and a floating rectangular cylinder.

Lassiter (1972), using the variational approach, studied waves normally incident on a rectangular trench where the water depths before and after the trench are constant but not necessarily equal, referred to here as the asymmetric case. Lee &

Ayer (1981) employed a transform method to obtain a solution for the case of propagation of normally incident waves over a symmetric rectangular trench; explicit solutions are obtained in the constant-depth region and the region of the trench, which are then matched numerically. Kreisel (1949) presented a general analysis for obstacles of finite extent and suitable geometry which proceeds by mapping the two-dimensional fluid domain into a rectangular strip; the velocity potential is then obtained by solving a linear integral equation by iteration. Miles (1982) obtained results for normally incident long waves in the symmetric case, using the mapping procedure of Kreisel (1949); corrections to the reflection and transmission coefficients for oblique wave incidence are obtained based on the variational formulation of Mei & Black (1969).

Our aim in the present study is to extend the results for the rectangular trench to the case of large angles of incidence and asymmetric geometry. Of special interest will be the case where the wavenumber component for the incident wave in the direction of the trench axis exceeds the wavenumber for the propagating modes in the trench; in this case the solutions for modes with exponential depth dependence in the trench vary sinusoidally along the trench axis but exponentially in the cross-trench direction. For a sloping step and waves propagating from shallow to deep water, this situation leads to the presence of a linear caustic and total reflection of the incident waves; for the sudden depth discontinuity studied here, rays of the incident wave field would be reflected at the discontinuity in depth. However, owing to the finiteness of the obstacle, transmitted waves appear on the downwave side of the trench in the geometric shadow region.

After formulating the problem in §2, we present in §3 results based on numerical solution of a set of integral equations derived using a modified form of Takano's method. Solutions are compared with previous results for normally incident waves, and several results are presented for normal- and oblique-incidence cases. Also, results of a small-scale experiment are presented in comparison with the theoretical predictions. In §4, we present an approximate solution involving consideration of only the plane-wave modes of the particular solutions for each region; explicit forms for reflection and transmission coefficients are obtained. We then obtain the long-wave asymptote of the plane-wave solution and compare our results with those of Miles (1982) for normal and oblique incidence.

2. The boundary-value problem

We consider the monochromatic small-amplitude motion of an inviscid, irrotational fluid with a free surface. The fluid domain is shown in figure 1. A coordinate system is established with z positive upwards and equal to zero at the free surface, and the y-axis extending along the trench boundary on the incident wave side. The depths are constant in each region, and in general differ, with the restriction that the depth in region 2 (the trench) must not be less than that in either region 1 or 3.

We wish to investigate the diffraction of a plane surface wave incident from infinity in region 1, whose direction of propagation forms an angle θ_1 with the x-axis in region 1. The wave is affected by the trench in region 2, and there is a decaying or transmitted wave in region 3. The velocity potential $\tilde{\phi}(x,y,z,t)$ must satisfy Laplace's equation

$$\nabla^2\tilde{\phi} = 0, \quad \nabla^2 = \left\{\frac{\partial^2}{\partial x^2} + \frac{\partial^2}{\partial y^2} + \frac{\partial^2}{\partial z^2}\right\}, \tag{2.1}$$

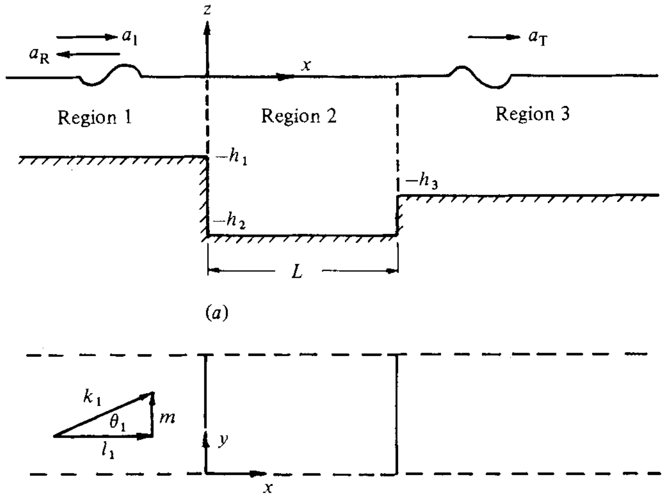

FIGURE 1. Definition sketch. (a) vertical section, (b) plan.

in the entire fluid domain, together with a free-surface boundary condition

$$\frac{\partial \tilde{\phi}}{\partial z} + K\tilde{\phi} = 0, \quad K = \frac{\sigma^2}{g} \quad (z = 0). \tag{2.2}$$

Here σ is the angular frequency of the monochromatic motion. No-flow conditions on the solid boundaries give

$$\frac{\partial \tilde{\phi}}{\partial \boldsymbol{n}} = 0, \tag{2.3}$$

where $\boldsymbol{n}$ is the outward normal to any of the fixed boundary segments in figure 1. Reflected and transmitted waves in regions 1 and 3 respectively must also satisfy radiation conditions at $x = \pm\infty$.

Anticipating the form of particular solutions, we denote the wavenumber of the incident wave in region 1 by k_1, and let m be given by

$$m = k_1 \sin\theta_1,$$

the projection of the incident wavenumber along the y-axis. Consideration of the phase speed along rays of the incident wave leads to Snell's law for refraction across discontinuities in the water depth, resulting in

$$m = k_i \sin\theta_i = \text{constant} \quad (i = 1, 2, 3).$$

The velocity potentials $\tilde{\phi}_i(x, y, z, t)$ in each region may then be written as

$$\tilde{\phi}_i(x, y, z, t) = \phi_i(x, z)\, e^{i(my - \sigma t)} \quad (i = 1, 2, 3). \tag{2.4}$$

Solutions of the reduced boundary-value problem given by (2.1) together with the boundary conditions (2.2) and (2.3) and the radiation conditions at $x = \pm\infty$ may be constructed from the particular solutions in each region of the fluid domain:

$$\phi_i(x, z) = A_i^{\pm}\, \chi_i(z)\, e^{\pm i l_i x} + \sum_{n=1}^{\infty} B_{i,n}^{\pm}\, \psi_{i,n}(z)\, e^{\pm \lambda_{i,n} x} \quad (i = 1, 2, 3), \tag{2.5}$$

where
$$\lambda_{i,n} = (\kappa_{i,n}^2 + m^2)^{\frac{1}{2}},$$
$$l_i = \mathrm{i}\lambda_{i,0} = (k_i^2 - m^2)^{\frac{1}{2}}.$$

Here $A_1^+ = 1$, $A_1^- = A_R$, $A_3^+ = A_T$ are the coefficients of the incident, reflected and transmitted waves respectively. In addition, we may take A_3^-, $B_{1,n}^-$ and $B_{3,n}^+ = 0$ for $n = 1, \ldots, \infty$.

The associated dispersion relations are given by

$$K + \kappa_i \tan \kappa_i h_i = 0 \quad (i = 1, 2, 3). \tag{2.6}$$

Equations (2.6) have an infinite discrete set of real roots $\pm\kappa_{i,n}$, and a pair of imaginary roots $\pm k_i = \pm \mathrm{i}\kappa_{i,0}$. The functions $\psi_{i,n}$ and χ_i are given by

$$\psi_{i,n} = \cos \kappa_{i,n}(h_i + z) \quad (n = 1, \ldots, \infty), \tag{2.7a}$$

$$\chi_i = \psi_{i,0} = \cosh k_i(h_i + z) \quad (i = 1, 2, 3). \tag{2.7b}$$

and form a complete orthogonal set over the depth in each region. The $\psi_{i,n}$ correspond to non-propagating wave modes, while the χ_i represent the free wave modes.

It is possible, for a range of values of θ_1 and h_2/h_1, to obtain the condition $m > k_2$, in which case the boundary between regions 1 and 2 becomes reflective to the incident plane wave, and the waveforms corresponding to $A_2^{\pm}$ change from sinusoidal to exponential dependency in the cross-trench direction. In this case, the presence of a second barrier at $x = L$, with $m < k_3$, allows for transmission in region 3. In the event that $m > k_3$, total reflection occurs.

In the special case when $l_2 = m$, ϕ_2 assumes the form

$$\phi_2(x, z) = \{A_2 + A_2' x\}\chi_2(z) + \sum_{n=1}^{\infty} B_{2,n}^{\pm}\psi_{2,n}(z)\,\mathrm{e}^{\pm\lambda_{2,n}x},$$

which represents the non-propagating modes plus a free wave travelling along the trench with constant or linearly varying amplitude across the trench. In the case of an infinitely wide trench (or when $h_3 = h_2$), A_2' must be set equal to zero owing to the requirement of boundedness as $x \rightarrow \infty$. For a trench of finite width, A_2' is in general non-zero.

Solutions to the full problem must satisfy certain matching conditions over the vertical planes separating the fluid regions, namely

$$\phi_1 = \phi_2, \quad \frac{\partial \phi_1}{\partial x} = \frac{\partial \phi_2}{\partial x} \quad (x = 0;\ -h_1 \leqslant z \leqslant 0), \tag{2.8a, b}$$

$$\phi_2 = \phi_3, \quad \frac{\partial \phi_2}{\partial x} = \frac{\partial \phi_3}{\partial x} \quad (x = L;\ -h_3 \leqslant z \leqslant 0). \tag{2.9a, b}$$

These conditions provide continuity of pressure and horizontal velocity normal to the vertical fluid boundaries.

An incident wave with amplitude a_I given by

$$a_I = g^{-1}\sigma \cosh k_1 h_1 \tag{2.10}$$

is presumed to be incident from $x = -\infty$ in region 1, with reflected and transmitted wave amplitudes given respectively by

$$a_R = g^{-1}\sigma |A_R| \cosh k_1 h_1; \quad a_T = g^{-1}\sigma |A_T| \cosh k_3 h_3. \tag{2.11a, b}$$

Reflection and transmission coefficients are then given by

$$\left.\begin{aligned} &K_{\mathrm{T}} = |A_{\mathrm{T}}|\frac{\cosh k_3 h_3}{\cosh k_1 h_1}, \quad K_{\mathrm{R}} = |A_{\mathrm{R}}| \quad (l_3 \text{ real}),\\ &K_{\mathrm{T}} = 0,\ K_{\mathrm{R}} = 1\ (l_3 \text{ imaginary}). \end{aligned}\right\} \tag{2.12a, b}$$

Conservation of energy in the diffracted wave field leads to the condition that

$$K_{\mathrm{R}}^2 + K_{\mathrm{T}}^2\left\{\frac{n_3 k_1^2 l_3}{n_1 k_3^2 l_1}\right\} = 1 \tag{2.13}$$

in the general case, where

$$n_i = \frac{1}{2}\left(1+\frac{2k_i h_i}{\sinh 2k_i h_i}\right) \quad (i = 1, 2, 3).$$

This condition was found to be satisfied automatically by the solutions discussed in §§3 and 4.

3. Numerical solution and results

Takano (1960) constructed a solution to the problem of wave transmission over an elevated rectangular sill based on eigenfunction expansions of the form (2.4), with the restriction that $\theta_1 = 0$. The expansions for each region are matched at the vertical boundaries according to the conditions (2.8) and (2.9). The method then proceeds by constructing a theoretically infinite set of independent integral equations by multiplying in turn each matching condition by all members of one of the sets $\{\psi_{i,n};\ n = 0, \ldots, \infty\}$ and integrating each resulting equation over the appropriate depth. The choice of the set of eigenfunctions to be used with each matching condition depends on the geometry of the domain; here, the order of the choice of sets is reversed from the order used by Takano, as required by the shift from an elevated obstacle to a trench. This accounts for the restriction $h_2 \geqslant \{h_1, h_3\}$.

3.1. *Formulation and solution technique*

In order to construct a solution, it is first necessary to truncate the infinite series in (2.4) to a finite number of terms given by N. We then must solve for $4N+4$ unknown coefficients A_{R}, $A_2^{\pm}$, A_{T}, $B_{1,n}^{+}$, $B_{2,n}^{\pm}$, $B_{3,n}^{-}$ $(n = 1, \ldots, N)$. Matching and boundary conditions are manipulated in the following manner. First, we consider the condition of continuity of normal derivatives for ϕ for the vertical boundaries at $x = 0, L$, given by (2.8b) and (2.9b). Making use of the orthogonality of the set $(\chi_{2,n}(z);\ n = 0, \ldots, N\}$ in region 2, we construct $2N+2$ integral equations of the form

$$\begin{aligned} \int_{-h_1}^{0} \frac{\partial \phi_1}{\partial x}(0,z)\,\psi_{2,n}(z)\,\mathrm{d}z &= \int_{-h_1}^{0} \frac{\partial \phi_2}{\partial x}(0,z)\,\psi_{2,n}(z)\,\mathrm{d}z \\ &= \int_{-h_2}^{0} \frac{\partial \phi_2}{\partial x}(0,z)\,\psi_{2,n}(z)\,\mathrm{d}z \quad (n = 0, \ldots, N), \end{aligned} \tag{3.1a}$$

$$\begin{aligned} \int_{-h_3}^{0} \frac{\partial \phi_3}{\partial x}(L,z)\,\psi_{2,n}(z)\,\mathrm{d}z &= \int_{-h_3}^{0} \frac{\partial \phi_2}{\partial x}(L,z)\,\psi_{2,n}(z)\,\mathrm{d}z \\ &= \int_{-h_2}^{0} \frac{\partial \phi_2}{\partial x}(L,z)\,\psi_{2,n}(z)\,\mathrm{d}z \quad (n = 0, \ldots, N), \end{aligned} \tag{3.1b}$$

N	$k_1 h_1 = 0.341$ K_T	K_R	$k_1 h_1 = 0.723$ K_T	K_R	$k_1 h_1 = 1.296$ K_T	K_R
2	0.8900	0.4559	0.9552	0.2961	0.9992	0.0404
4	0.8889	0.4582	0.9554	0.2955	0.9994	0.0332
8	0.8884	0.4590	0.9552	0.2961	0.9995	0.0324
16	0.8882	0.4595	0.9552	0.2961	0.9995	0.0310
32	0.8881	0.4596	0.9552	0.2960	0.9995	0.0306

TABLE 1. Values of K_T and K_R computed for different values of N; $h_3 = h_1$, $h_2/h_1 = 3$, $L/h_1 = 10$, $\theta = 0°$

where the shift of integration limits in the last terms is possible since there is no contribution to the horizontal velocity field from the contours $(-h_2 \leqslant z < -h_1;\ x = 0)$, $(-h_2 \leqslant z < -h_3;\ x = L)$.

Similarly, a second set of $2N+2$ equations is constructed from the condition for continuity of pressure. Here we are only concerned with the pressure over the vertical strips $(-h_1 \leqslant z \leqslant 0;\ x = 0)$ and $(-h_3 \leqslant z \leqslant 0;\ x = L)$. In this case we take advantage of the orthogonal properties of the sets $\psi_{1,n}$, $\psi_{3,n}$ $(n = 0, \ldots, N)$. The integral equations are given by

$$\int_{-h_1}^{0} \phi_1(0,z)\, \psi_{1,n}(z)\, \mathrm{d}z = \int_{-h_1}^{0} \phi_2(0,z)\, \psi_{1,n}(z)\, \mathrm{d}z \quad (n = 0, \ldots, N), \tag{3.2a}$$

$$\int_{-h_3}^{0} \phi_3(L,z)\, \psi_{3,n}(z)\, \mathrm{d}z = \int_{-h_3}^{0} \phi_2(L,z)\, \psi_{3,n}(z)\, \mathrm{d}z \quad (n = 0, \ldots, N). \tag{3.2b}$$

The resulting set of $4N+4$ simultaneous equations (3.1), (3.2) are solved numerically as a linear matrix equation. Solution accuracy was checked by verifying that enough non-propagating wave modes were retained to give reasonable convergence of the transmission and reflection coefficients. For the purposes of our study it was determined that the choice of $N = 16$ produced sufficiently accurate results for most values of $k_1 h_1$; sample calculations are presented in table 1.

3.2. *Comparison with previous results*

Results applicable to the present study have been presented by Lee & Ayer (1981) for the case of a symmetric trench, and by Lassiter (1972) for symmetric and asymmetric trenches. Both studies are restricted to the case of normal wave incidence.

Our results are compared in figure 2 to points taken from figures 3 and 4 of Lee & Ayer (1981), for the geometry $h_2/h_1 = 7.625$, $L/h_1 = 5.28$, and for the choice $N = 16$. Present results agree closely with those of Lee & Ayer, with the only noticeable discrepancy occurring in the reflection coefficient for the range $0.7 \leqslant k_1 h_1 \leqslant 1.1$.

A comparison with the results of Lassiter (1972) is shown in figure 3, where K_R is plotted against Kh_1 rather than $k_1 h_1$. The results of the two methods are seen to disagree, particularly in the prediction of the value of Kh_1 corresponding to the first minimum of K_R. Lee & Ayer (1981) showed, but did not discuss, a similar disagreement in the symmetric case; however, the shift in Kh_1 found here is approximately four times larger than in the symmetric case.

In order to verify the trend of the present results, an independent solution was developed based on a boundary-integral method (BIM) identical with that of

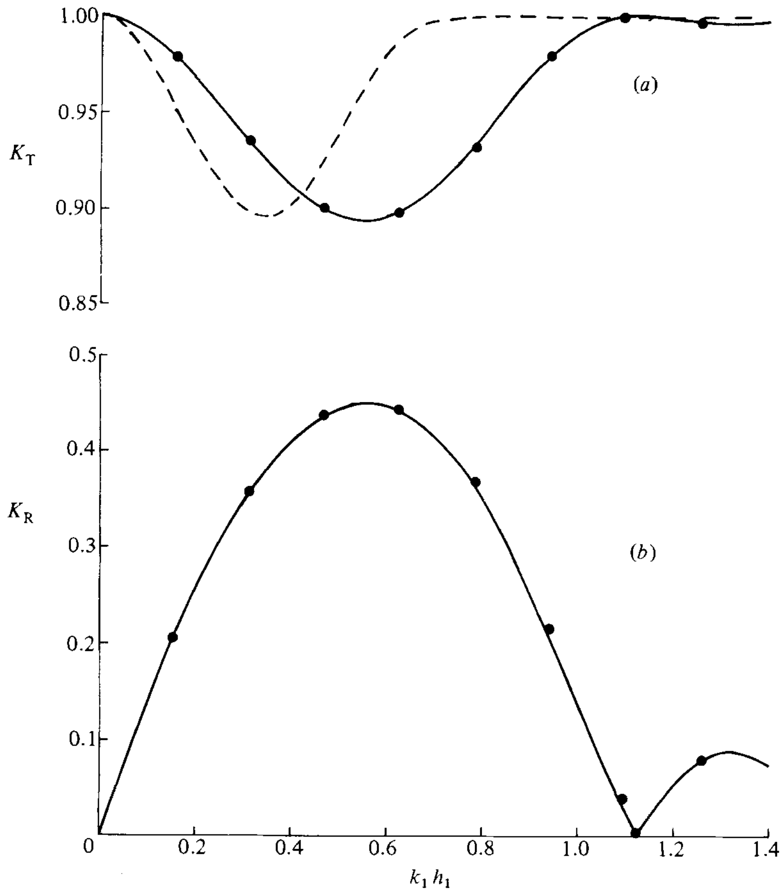

FIGURE 2. Transmission and reflection coefficients; $h_2/h_1 = 7.625$, $L/h_1 = 5.28$, $\theta_1 = 0$; ——, numerical solution; ●, data from Lee & Ayer (1981, figures 3 and 4); ----, plane-wave solution (4.4*b*).

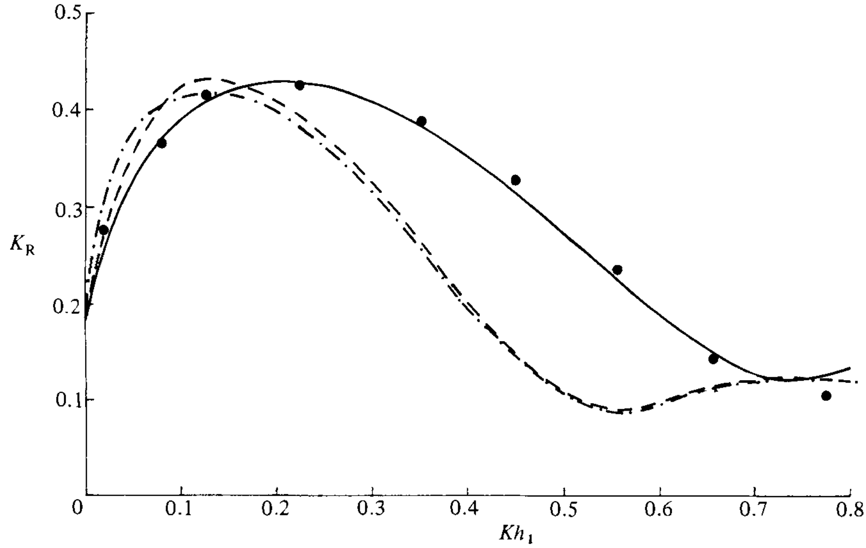

FIGURE 3. Reflection coefficient; $h_2/h_1 = 2$, $h_3/h_1 = 0.5$, $L/h_1 = 5$, $\theta_1 = 0$; ——, numerical solution ---, —·— results of Lassiter (1972, figure 7); ●, BIM solution.

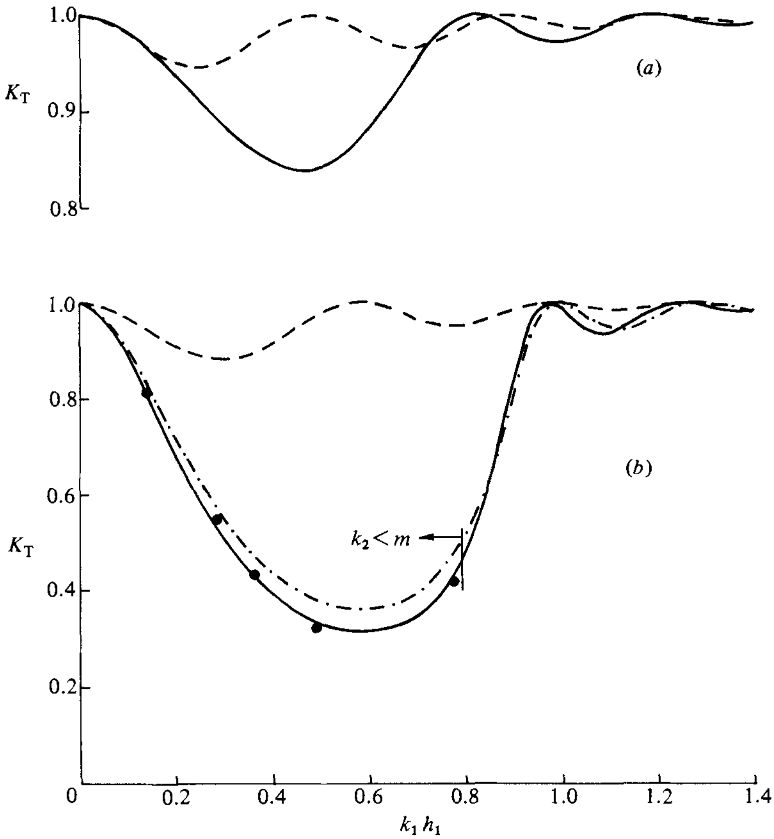

FIGURE 4. Transmission coefficient, symmetric case, two angles of incidence; $L/h_1 = 10$: (*a*) $h_2/h_1 = 2$; (*b*) $h_2/h_1 = 3$, $l_2 = 0$ at $k_1 h_1 = 0.792$. ----, numerical solution, $\theta_1 = 0$. ——, numerical solution; —·—·, plane-wave solution (4.4*b*); ●, BIM solution; $\theta_1 = 45°$.

Raichlen & Lee (1978), also utilized by Lee & Ayer (1981). The asymmetry of the problem was accommodated by taking the closed boundary to enclose the entire trench and a region of one trench width to either side. Results obtained using a relatively cruder boundary discretization than used by Lee & Ayer (1981) are shown in figure 3, and verify the trend of the present solution in comparison with Lassiter's (1972) results.

3.3. *Results for normal and oblique incidence*

Results for two cases using a symmetric trench ($h_1 = h_3$) are shown in figure 4, where we demonstrate the effect of increasing the trench depth (for a fixed incidence wave angle) to the point where l_2 is imaginary for a range of values of $k_1 h_1$ for the incident wave, with $\theta_1 = 0°$ and $45°$. For both depths, the trench width is equivalent ($L/h_1 = 10$), while the trench depths are given by $h_2/h_1 = 2$ in figure 4(*a*) and $h_2/h_1 = 3$ in figure 4(*b*). For the 45° angle of incidence, l_2 approaches 0 in the limit $k_1 h_1 \rightarrow 0$ in figure 4*a*; this does not affect the solution in any significant way. In figure 4(*b*) for a 45° angle of incidence, the solution passes through the point $l_2 = 0$ at a value of $k_1 h_1 = 0.792$. The reduction in transmission across the trench caused by the theoretical presence of a totally reflective local barrier at $x = 0$ is clear, with K_T dropping to a minimum of 0.31. The transmission coefficient recovers to unity in the limit $k_1 h_1 \rightarrow 0$ owing to the vanishing width of the trench relative to the incident wavelength.

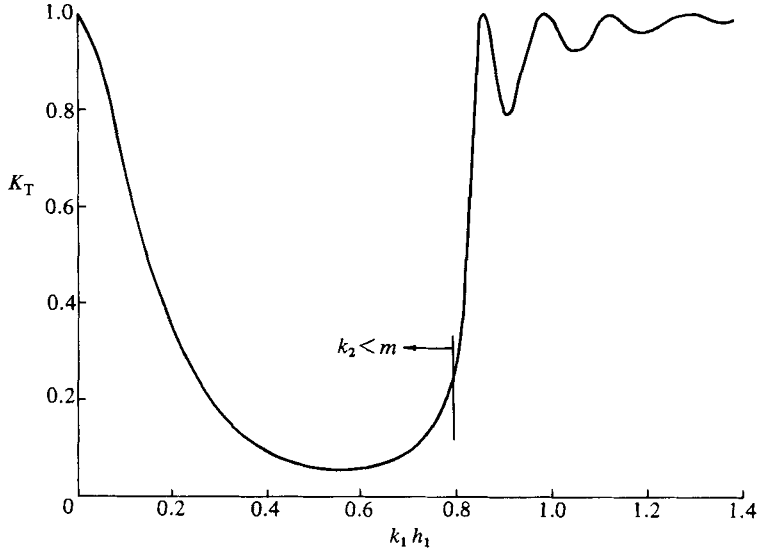

FIGURE 5. Transmission coefficient, symmetric case; $L/h_1 = 20$, $h_2/h_1 = 3$, $\theta_1 = 45°$. ——, numerical solution, $l_2 = 0$ at $k_1 h_1 = 0.792$.

Results obtained by modifying Raichlen & Lee's (1978) BIM formulation to the case of oblique incidence are shown also in figure 4(*b*). Again these results are obtained using a relatively crude boundary discretization, and serve to verify the trend of the numerical solution described above. The BIM is modified by incorporating the Green function for the modified Helmholtz equation obtained by substituting (2.4) in (2.1). A similar method, using a more refined boundary discretization technique, has been utilized by Liu & Abbaspour (1982) to study the diffraction of oblique waves by floating cylinders.

In figure 5 the effect of increasing the trench width at a fixed depth ratio is demonstrated for the case $L/h_1 = 20$, $h_2/h_1 = 3$. The position of $l_2 = 0$ is unchanged from figure 4(*b*). The minimum value of K_T drops significantly below that given in the previous figure; it is apparent that K_T would indeed approach zero for l_2 imaginary for increasingly wider trenches.

In order to further verify the nature of the solutions in the range of l_2 imaginary, an experiment was conducted in a small 4 ft × 8 ft wave basin. A $4\frac{1}{8}$ in. deep trench was constructed at a 45° angle to a single-flap wave generator. A border of 4 in. thick glued fibres was placed around the perimeter of the basin in order to reduce reflections. A depth of $h_1 = 1\frac{1}{8}$ in. was chosen for the experimental tests; the physical dimensions were given by $h_2/h_1 = 4.56$ and $L/h_1 = 8.67$. Only the symmetric case was tested. For this condition, $l_2 = 0$ at a value of $k_1 h_1 = 0.871$. Data were collected for the range of $0.58 < k_1 h_1 < 0.96$, covering the range of transition from propagating to standing waves in the cross-trench direction. Transmission coefficients were determined by comparing the transmitted wave height in the presence of the trench with that obtained by covering the trench. Results are shown in figure 6 in comparison with the numerical predictions. It was found that, for values of $k_1 h_1 < 0.58$, the wave field contained too many reflected components to make an adequate resolution of the desired results possible; for the range of $k_1 h_1$ values tested, reflections from the fibre mats were on the order of 5% of the incident amplitude. For values of $k_1 h_1$ above the range tested, the wave field is dominated by progressive waves in the trench, and we would not expect the results to differ qualitatively from

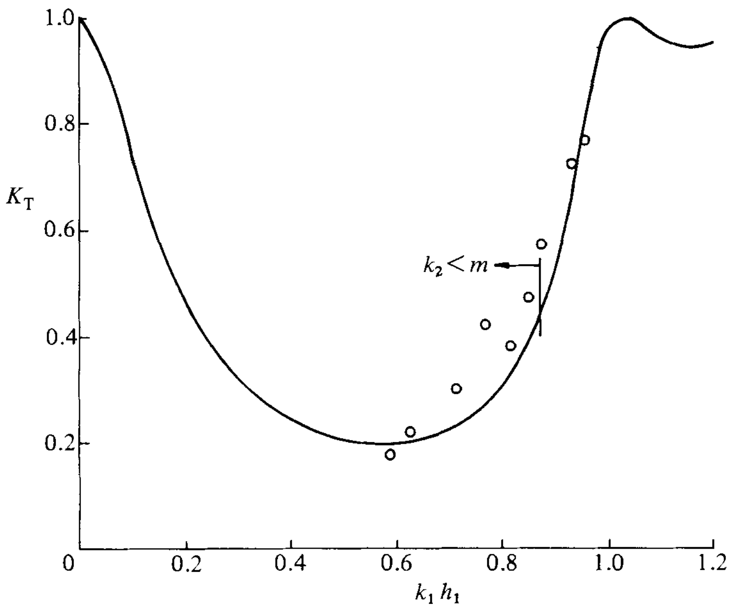

FIGURE 6. Transmission coefficient, symmetric case; $L/h_1 = 8.67$, $h_2/h_1 = 4.56$, $\theta_1 = 45$, $l_2 = 0$ at $k_1 h_1 = 0.871$: ——, numerical results; ○, experimental results.

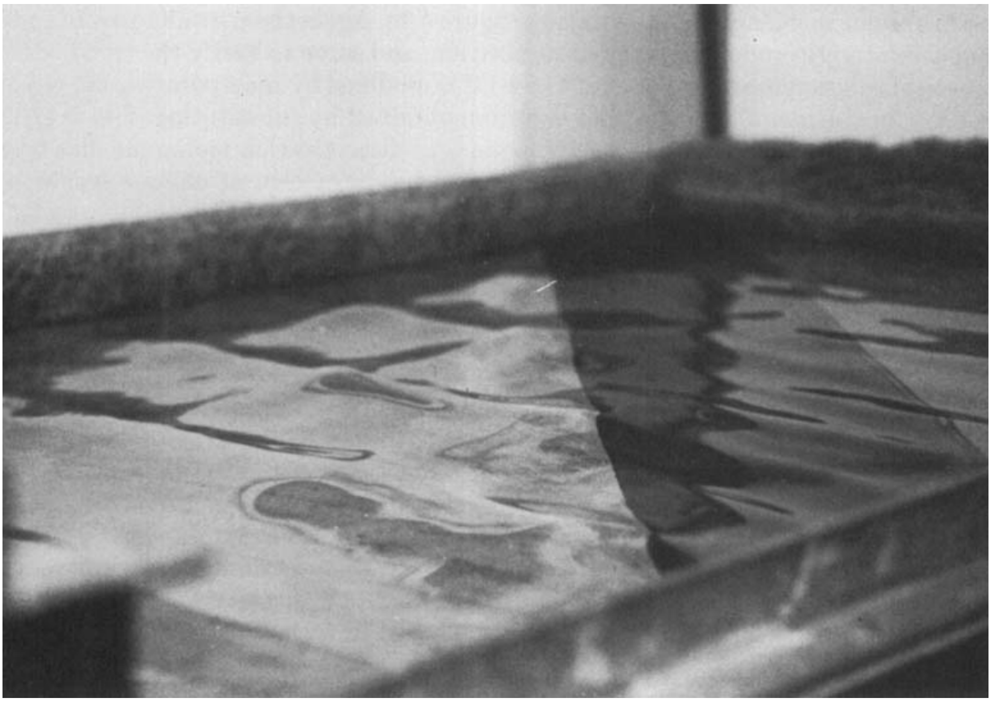

FIGURE 7. Experimental wave pattern. Case of figure 6, $k_1 h_1 = 0.85$. Trench appears as dark band, with waves incident from the lower left. Reflected wave propagates towards upper left.

the data of Lee & Ayer (1981). From the results presented here, it was concluded that the theory accurately predicts the behaviour of the wave field in the transition from progressive to standing modes in the trench.

An example wave field is shown in figure 7, for the case $k_1 h_1 = 0.85$. Here the amplitude of the incident wave has been increased for the sake of clarity, leading to

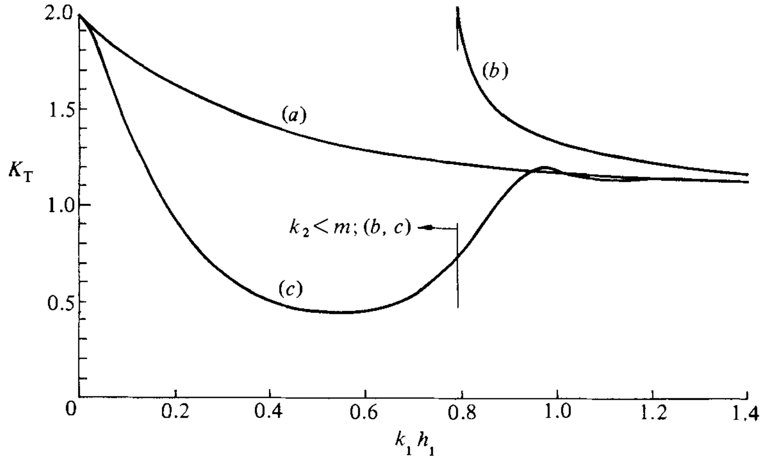

FIGURE 8. Transmission coefficient, asymmetric cases. Results of numerical model, $\theta_1 = 45°$, $L/h_1 = 10$. (a) $h_2 = h_3 = 2h_1$; (b) $h_2 = h_3 = 3h_1$, $l_2 = l_3 = 0$ at $k_1 h_1 = 0.792$; (c) $h_2/h_1 = 3$, $h_3/h_1 = 0$, $l_2 = 0$ at $k_1 h_1 = 0.792$.

the presence of free harmonic components which are visible as part of the transmitted wave (to the right in the figure). The reflection of the incident wave (from the left) is clearly shown upwave of the trench (dark band in photo).

Results for several asymmetric cases and an angle of incidence $\theta_1 = 45°$ are shown in figure 8. Case (*a*) represents the transmission of waves over a single step, with $h_3 = h_2 = 2h_1$, and $l_2 (= l_3)$ real for all finite values of $k_1 h_1$. In this case K_T approaches a value of 2 in the limit of small $k_1 h_1$, and decays monotonically to a value of 1 as $k_1 h_1$ increases. For case (*b*), where $h_3 = h_2 = 3h_1$, K_T also approaches 1 monotonically for large $k_1 h_1$; however, the asymptotic value of 2 is approached as $k_1 h_1 \rightarrow 0.792$, where $l_2 = l_3 = 0$. For smaller values of $k_1 h_1$ no transmission is possible.

Case (*c*) represents an asymmetric trench, with $h_2/h_1 = 3$, $h_3/h_1 = 2$ and $L/h_1 = 10$. As in figure 4(*b*), l_2 takes imaginary values for $k_1 h_1$ less than 0.792, while transmitted waves are free to propagate in region 3 for all values of $k_1 h_1$. In the range $0 < k_1 h_1 < 0.792$, the solution appears to be dominated by the characteristics of the trench, although the reduction of K_T is not as large as seen in figure 4(*b*), owing to the lower step occurring at $x = L$. For $k_1 h_1 > 0.792$, the solution approaches the case (*a*) solution, indicating the dominance of region 3 in the short-wave limit. The approach of the case (*c*) solution to the case (*a*) solution is oscillatory, indicating the effect of interference between the two trench boundaries.

4. Plane-wave approximation and the long-wave limit

A long-wave approximation for the reflection and transmission of a plane wave normally incident at a step was first given by Lamb (1932), who constructed a solution by matching surface displacement and the mass flux normal to the depth discontinuity. Bartholomeuz (1958) found that this solution, while disregarding the requirement of no normal velocity over the vertical face of the step, gave the correct lowest order (in *kh*) results for the reflection and transmission coefficients. Miles (1967) pointed out that Lamb's assumptions are equivalent to neglecting the non-propagating modes with eigenfunctions $\psi_{i,n}$ in the limit of small $k_i h_i$. Miles then constructed a plane-wave solution for unrestricted values of *kh* for the case of propagation over a single step, studied by Newman (1965*b*) and found that the resulting approximation for K_T agreed with Newman's results to within 5% for all values of *kh*.

In this section we derive an approximate solution for the asymmetric case $h_1 \neq h_3, h_2 \geqslant \max(h_1, h_3)$, based on the plane-wave modes. It is again noted that, in the case of $l_2(=(k_2^2-m^2)^{\frac{1}{2}})$ imaginary, it is necessary to retain the exponentially decaying modes A_2^+ and A_2^- in (3.16) as part of the formulation. After obtaining explicit results for the values of A_T and A_R for the general case of oblique incidence at an asymmetric trench, we take the limit for small kh to obtain results which are consistent with Lamb's level of approximation.

4.1. *Plane-wave approximation*

For the plane-wave approximation, we consider simplified versions of the velocity potentials (2.5) in each region given by

$$\phi_1(x,z) = \chi_1(z)\{e^{il_1x} + A_R e^{-il_1x}\}, \tag{4.1a}$$

$$\phi_2(x,z) = \chi_2(z)\{A_2^+ e^{il_2x} + A_2^- e^{-il_2x}\}, \tag{4.1b}$$

$$\phi_3(x,z) = \chi_3(z) A_T e^{il_3x}. \tag{4.1c}$$

Corresponding matching conditions are obtained by neglecting all terms containing $\psi_{i,n}$ $(n > 0)$ in (3.1), (3.2). Solving for the reflected and transmitted waves, we obtain the results

$$A_R = \frac{(\alpha'\beta-\alpha\beta')\cos l_2 L + i(\alpha\alpha'-\beta\beta')\sin l_2 L}{-(\alpha'\beta+\alpha\beta')\cos l_2 L + i(\alpha\alpha'+\beta\beta')\sin l_2 L} \tag{4.2a}$$

for the reflected wave, and

$$A_T = \frac{2\alpha\beta(I_2/I_1)e^{-il_3L}}{(\alpha'\beta+\alpha\beta')\cos l_2 L - i(\alpha\alpha'+\beta\beta')\sin l_2 L} \tag{4.2b}$$

for the transmitted wave, where

$$\alpha = l_1 I_1^2, \quad \alpha' = l_3 I_2^2, \quad \beta = l_2 I_3 I_4, \quad \beta' = l_2 I_3 I_5, \tag{4.3}$$

and

$$I_1 = \int_{-h_1}^{0} \chi_1(z)\chi_2(z)\,dz, \quad I_2 = \int_{-h_3}^{0} \chi_3(z)\chi_2(z)\,dz,$$

$$I_3 = \int_{-h_2}^{0} \chi_2^2(z)\,dz, \quad I_4 = \int_{-h_1}^{0} \chi_1^2(z)\,dz, \quad I_5 = \int_{-h_3}^{0} \chi_3^2(z)\,dz.$$

For the symmetric case ($h_1 = h_3$, $\alpha = \alpha'$, $\beta = \beta'$) the reflection and transmission coefficients reduce to

$$K_R^2 = \frac{A}{1+A}, \tag{4.4a}$$

$$K_T^2 = \frac{1}{1+A}, \tag{4.4b}$$

where

$$A = \frac{(\alpha^2-\beta^2)^2}{4\alpha^2\beta^2}\sin^2 l_2 L.$$

This result is analogous to the result from quantum mechanics for the linear tunnelling of a free particle with energy $E = \alpha^2$ through a barrier of width L and potential $V_0 = \alpha^2 - \beta^2$ (see e.g. Anderson 1971, §5.2). It is notable that the case of a classically impenetrable barrier, with $V_0 > E$, corresponds to the range where l_2 assumes imaginary values. It is in this range that the geometric-optics approximation for water waves would preclude transmitted waves even in the case of a finite barrier width.

It is apparent from (4.4) that the approximate solution conserves energy identically. The incident wave is completely transmitted for all l_2 when $\alpha = \beta$, which is satisfied when $h_1 = h_2$. In the limit $l_2 \to 0$, β also vanishes; writing out the terms in (4.4*b*), we obtain

$$K_{\mathrm{T}}^2 = \left(1 + \frac{l_1^2 I_1^4}{4 I_3^2 I_4^2} L^2\right)^{-1} \quad (l_2 = 0). \tag{4.5}$$

For l_2 imaginary (4.4*b*) rewritten in terms of real quantities gives

$$K_{\mathrm{T}}^2 = \left(1 + \frac{(\alpha^2 + |\beta|^2)^2}{4\alpha^2|\beta|^2} \sinh^2 |l_2| L\right)^{-1} \quad (l_2 \text{ imaginary}). \tag{4.6}$$

For both of these cases, it is evident that the transmitted wave vanishes as $L \to \infty$, as expected. Complete transmission also takes place (for l_2 real) whenever

$$l_2 L = n\pi \quad (n = 0, 1, 2, \ldots). \tag{4.7}$$

The case $n = 0$ is again a trivial solution corresponding to the case of a trench of vanishing width in comparison to the wavelength. For $n > 0$, complete transmission occurs whenever the trench width is equal to an integer number of half-wavelengths in the x-direction, given by π/l_2. This result is valid for shallow water; however, it has been shown by Newman (1965*a*) to be an incorrect result for waves in water of arbitrary depth. For the full problem, complete transmission would be expected to occur at wave conditions where

$$l_2 L = n\pi + \delta_{\mathrm{r}}, \tag{4.8}$$

where δ_{r} represents a phase shift for reflection of waves in the trench. The effect of this phase shift can become dramatic for large values of h_2/h_1 – see figure 2(*a*) and the discussion below.

For the case of a single step, we set $h_2 = h_3 > h_1$. Equations (4.2*a*, *b*) then reduce to

$$A_{\mathrm{R}} = \frac{\alpha - \beta}{\alpha + \beta}, \quad A_{\mathrm{T}} = \frac{2\alpha\beta I_2/I_1}{\alpha'(\alpha + \beta)}, \tag{4.9}$$

which are analogous to equation (4.8) of Miles (1967). For $\beta = 0$ ($l_2 = 0$), we obtain the result $A_{\mathrm{R}} = 1$, $A_{\mathrm{T}} = 2I_4/I_1$. For β (or l_2) imaginary, we obtain

$$|A_{\mathrm{R}}| = 1, \quad |A_{\mathrm{T}}| = 2\frac{I_4}{I_1}\frac{\alpha}{(\alpha^2 + |\beta|^2)^{\frac{1}{2}}}. \tag{4.10}$$

Here we must reinterpret (3.4*a*) for the case l_3 ($= l_2$) imaginary. Since it is clear that A_{T} is the coefficient of an exponentially decaying mode, it does not represent the propagation of wave energy into regions 2 and 3. Therefore $K_{\mathrm{T}} = 0$; both $\beta = 0$ and β imaginary give total reflection of the incident wave, as required.

Results of the plane-wave solution, shown in figure 4(*b*), indicate that the approximate solution yields reasonably accurate results for the relatively small depth differences studied here. This fortuitous result is seen to break down when the depth differences are increased. The plane-wave approximation was tested for a trench geometry corresponding to that of Lee & Ayer (1981, figure 3), with $h_2/h_1 = 7.625$ and $L/h_1 = 5.28$; results are shown in figure 2(*a*). The location of the first maximum of K_{T} is shifted drastically by the neglect of the non-propagating modes, even though the magnitude of the minimum value is predicted fairly well.

4.2. *The long-wave limit*

For the limit of small kh in all regions, the numerical and plane-wave solutions discussed above converge to a form analogous to Lamb's treatment. In particular, the velocity potentials for the full problem lose their modal structure; the dispersion relation (2.6) reduces to

$$K+\kappa_i^2 h_i = 0, \tag{4.11}$$

which admits only the pair of imaginary roots $\pm k_i$ given by

$$k_i = \sigma(gh_i)^{-\frac{1}{2}}.$$

In addition, the depth dependence $\psi_i(z) \rightarrow 1$. Forms for the reflection and transmission coefficients may be derived from the results of §4.1; in particular, for the symmetric case $(h_3 = h_1) \neq h_2$, the transmission coefficient is given by

$$K_T^2 = \left(1+\frac{(h_1^2 l_1^2 - h_2^2 l_2^2)^2}{4h_1^2 h_2^2 l_1^2 l_2^2}\sin^2 l_2 L\right)^{-1}. \tag{4.12}$$

Results for the symmetric case can be compared with the results of Miles (1982), who solved for the values of A_R and A_T (our notation) for both normal and oblique incidence. Miles' results for normal incidence were obtained using the mapping procedure developed by Kreisel (1949), and are limited to small values of kh in each region. Miles' results are further limited by the assumption that the wave phase varies only slightly over the length of the obstacle; this will be seen to be a severe limitation in one of our cases discussed below. Following our notation, Miles' results for the transmitted wave are given by

$$A_T = \frac{1}{1-ik_1 l}, \quad K_T^2 = \frac{1}{1+(k_1 h_1)^2 (l/h_1)^2}, \tag{4.13}$$

where l/h_1 is a dimensionless ratio; values of l/h_1 for fixed values of $\frac{1}{2}L/h_1$ and $(h_2-h_1)/h_1$ may be obtained from Miles (1982, figures 2 and 3, or directly from the analytic result). For small values of $k_1 h_1$ and correspondingly narrow trenches, results obtained using (4.13) were found to agree closely with the numerical solution of §3, with parameters $L/h_1 = 2$, 8 and $1 \leqslant h_2/h_1 \leqslant 2$ being tested. In contrast, results obtained using (4.4) or (4.12) were seen to deviate slightly from the numerical results for all values of $k_1 h_1$ investigated, indicating the importance of the neglected non-propagating modes. Results for $k_1 h_1 = 0.2$ are shown in figure 9. For the case of a narrow trench $(L/h_1 = 2)$, Miles' solution is seen to agree closely with the numerical results, while the plane-wave solution is seen to deviate slightly. For the case $L/h_1 = 8$, the magnitude of the deviation of the plane-wave solution is similar. However, Miles' solution shows a significant deviation from both the numerical and plane-wave solutions. Here the trench width is about 25.7 % of the incident wavelength, and the assumptions made in obtaining Miles' solution are violated.

For the case of oblique incidence, Miles obtained a solution using a modified form of Mei & Black's (1969) variational formulation; the modified form of the transmission coefficient may be written as (following Miles 1982, equation (4.27*b*))

$$K_T = \cos\left\{l_1 h_1\left[\frac{\tan^2\theta_1}{2}\left(\frac{h_2}{h_1}-1\right)\left(\frac{L}{h_1}\right)+\frac{l}{h_1}\right]\right\}, \tag{4.14}$$

valid for l_2 real. Results obtained from (4.14) and the plane-wave approximation (4.4), for the geometry $h_2/h_1 = 2$, $L/h_1 = 8$, are compared in figure 10.

Overall, plane-wave results agree reasonably well with Miles' (1982) solutions. For the geometries tested, assumption of an obstacle short in comparison to the incident

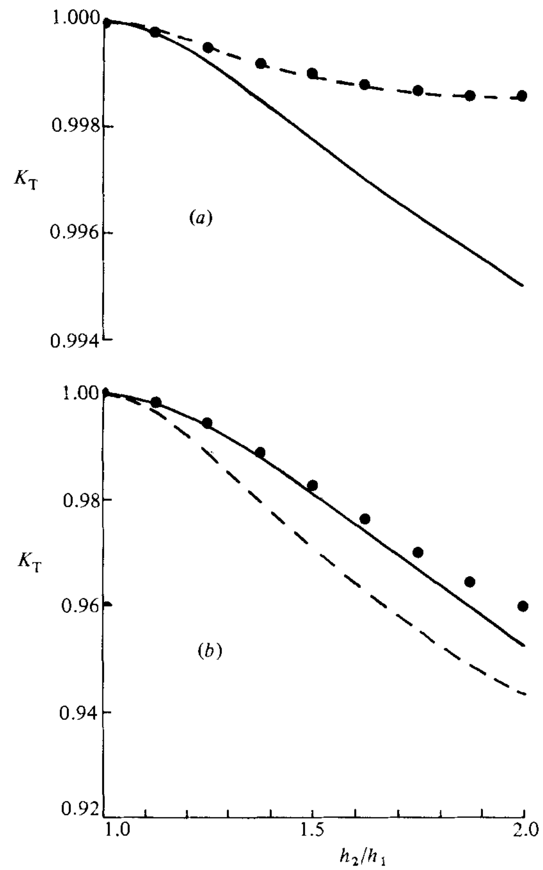

FIGURE 9. Transmission coefficient as a function of relative trench depth; normal incidence, $\theta_1 = 0$, $k_1 h_1 = 0.20$: (*a*) $L/h_1 = 2$; (*b*) $L/h_1 = 8$. ——, long-wave solution (4.12); ●, numerical results; ----, (4.13), after Miles (1982).

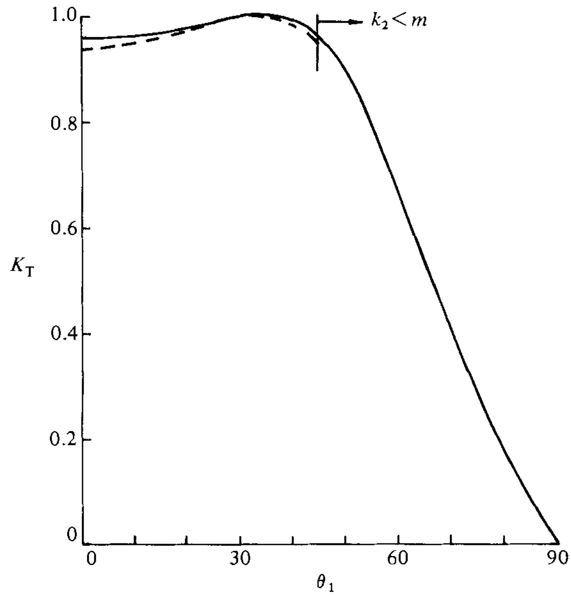

FIGURE 10. Transmission coefficient as a function of angle of incidence θ_1; $k_1 h_1 = 0.20$, $L/h_1 = 8$: ——, long-wave solution (4.12); ----, (4.14), after Miles (1982).

wavelength is seen to be more restrictive than the plane-wave approximation; however, the possibily drastic deviations of the plane-wave results from the numerical results for large values of kh were demonstrated above in the case of large relative-depth changes.

5. Concluding remarks

The analytic method used in §3 represents an extension to oblique angles of incidence of the method employed by Takano for the case of normally incident waves transmitted over an elevated sill. As was found by Newman (1965*b*), the use of such a method can lead to considerable computation requirements in the case of large differences in depths. In the present study, the result of principal interest, i.e. the large reduction in transmission caused by a local refractive barrier, could be discerned without recourse to large spatial differences in water depth. In the same sense, the relatively small depth differences allowed the approximate solutions formulated in §4 to produce results in rough qualitative agreement with the full solution; this qualitative agreement was seen to break down when results were compared with one case illustrated by Lee & Ayer (1981), where $h_2/h_1 = 7.625$, a much larger depth ratio than encountered in the present study.

The boundary integral method, used to verify the solutions in §3, represents a promising technique for extending the type of results obtained here to the case of irregular geometries. Results for one case have been presented by Lee, Ayer & Chang (1980), who studied a trapezoidal trench. The modification of Lee & Ayer's (1981) formulation to the case of an asymmetric geometry and oblique wave incidence, as in §3, allows for the study of an even greater variety of problems.

This work was supported in part by a grant from the Office of Naval Research, Coastal Science Program.

Note added in proof. Professors J. N. Newman and Dick K.-P. Yue have investigated the discrepancy between the results of Lassiter and the present study, as shown in figure 3. Using a finite-element technique, they have obtained results in qualitative agreement with those of the present study. The source of error in the original results of Lassiter is at present unknown.

REFERENCES

ANDERSON, E. E. 1971 *Modern Physics and Quantum Mechanics*. Saunders.

BARTHOLOMEUSZ, E. F. 1958 The reflexion of long waves at a step. *Proc. Camb. Phil. Soc.* **54**, 106–118.

KREISEL, G. 1949 Surface waves. *Q. Appl. Maths* **7**, 21–44.

LAMB, H. 1932 *Hydrodynamics*. Dover.

LASSITER, J. B. 1972 The propagation of water waves over sediment pockets. Ph.D. thesis, Massachusetts Institute of Technology.

LEE, J.-J. & AYER, R. M. 1981 Wave propagation over a rectangular trench. *J. Fluid Mech.* **110**, 335–347.

LEE, J.-J., AYER, R. M. & CHIANG, W.-L. 1980 Interactions of waves with submarine trenches. In *Proc. 17th Intl Conf. Coastal Engng, ASCE Sydney*, pp. 812–822.

LIU, P. L.-F. & ABBASPOUR, M. 1982 An integral equation method for the diffraction of oblique waves by an infinite cylinder. *Int. J. Num. Meth. Engng* **18**, 1497–1504.

MEI, C. C. & BLACK, J. L. 1969 Scattering of surface waves by rectangular obstacles in water of finite depth. *J. Fluid Mech.* **38**, 499–511.

MILES, J. W. 1967 Surface-wave scattering matrix for a shelf. *J. Fluid Mech.* **28**, 755–767.

MILES, J. W. 1982 On surface-wave diffraction by a trench. *J. Fluid Mech.* **115**, 315–325.

NEWMAN, J. N. 1965*a* Propagation of water waves past long two-dimensional obstacles. *J. Fluid Mech.* **23**, 23–29.

NEWMAN, J. N. 1965*b* Propagation of water waves over an infinite step. *J. Fluid Mech.* **23**, 399–415.

RAICHLEN, F. & LEE, J.-J. 1978 An inclined-plate wave generator. In *Proc. 16th Intl Conf. Coastal Engng, ASCE, Hamburg*, pp. 388–399.

SCHWINGER, J. & SAXON, D. S. 1968 *Discontinuities in Waveguides.* Gordon & Breach.

TAKANO, K. 1960 Effets d'un obstacle parallélépipédique sur la propagation de la houle. *Houille Blanche* **15**, 247–267.